# Gaussian Filters for P Class PMUs: a Performance Comparison of Alternative FIR Design Procedures

Xuansheng Shan[1,2], David Macii[2], He Wen[1], Dario Petri[2]
[1]*Hunan University - College of Electrical and Information Engineering,* Changsha, P.R. China
[2]*University of Trento - Dep. of Industrial Engineering*, Trento, Italy
E-mail: shanxs006@hnu.edu.cn, {david.macii, dario.petri}@unitn.it, he_wen82@126.com

***Abstract* — Protection-oriented (P Class) Phasor Measurement Units (PMUs) are required to estimate the synchrophasor, the frequency and the Rate of Change of Frequency (ROCOF) of ac voltage or current waveforms with high accuracy and low latency to detect possible anomalous events in power systems promptly and effectively. The classic architecture of many commercial PMUs relies on the direct frequency Down-Conversion and Filtering (DCF) of the collected input waveform. However, the adopted low-pass filters are generally optimized for harmonic disturbance rejection, while no much attention is usually devoted to overshoot minimization, which is instead of crucial importance when sudden phase or amplitude steps occur. Recalling that in principle the Gaussian filters exhibit zero-overshoot in the case of step changes, in this paper two alternative Finite Impulse Response (FIR) approximations of the Gaussian filter (one based on the windowing method and the other on the cascaded boxcar filters, respectively) are proposed and compared. Several simulation results (obtained in the P Class testing conditions of the IEEE/IEC Standard 60255-118-1:2018) confirm that both filters provide better results than those obtained with the classic triangular impulse response filter suggested in the Annex D of the Standard. Also, the results in the case of step changes exhibit almost zero overshoot and the same response times. However, due to the different frequency response in the stopband, the Gaussian filter approximation based on the cascade of boxcar filters provide slightly more accurate results than in the case when the windowing method is used, even though the latter provides a better approximation of the Gaussian impulse response.**

***Keywords—Phase Measurement Unit (PMU), Gaussian filter, Finite Impulse Response (FIR), boxcar filters, uncertainty.***

## I. INTRODUCTION

With the rapid diffusion of volatile renewable energy sources and distributed generation, the operating conditions of the power grids become more and more dynamic [1]. In this context, Power Measurement Units (PMUs) with high accuracy and low latency play a vital role in power systems monitoring and protection not only at the transmission level, but also at the distribution level [2, 3]. For this reason, a large diffusion of low-cost, high-accuracy PMUs is expected.

The Protection-oriented (P Class) PMUs are required to estimate synchrophasor with high accuracy and low latency in order to detect possible anomalous operating conditions promptly and effectively. To this end, a variety of estimation techniques based on digital signal processing have been used over the last few years. The classic Discrete Fourier Transform (DFT) algorithm is one of the simplest and most common approaches, and it is frequently used in practice, due to its low computational complexity and its inherent capability to reject harmonics in coherent sampling conditions. To improve the performance of DFT-based algorithms under frequency deviations and under the effect of narrowband interferers, several variants of the Interpolated DFT (IpDFT) exist [4-8]. However, the IpDFT approach inherently relies on static signal model. Therefore, it is not very suitable to track amplitude and phase oscillations changing dynamically over time. In order to improve the estimation accuracy under dynamic conditions, a model based on the Taylor's series expansion of the phasor was proposed in [9, 10]. The Taylor's series coefficients and, consequently, the synchrophasor amplitude and phase are then estimated by finding the least-squares solution of an overdetermined linear system, which relates the ideal signal model with the collected samples [11]. Following and extending the same approach, the so-called Taylor Fourier Transform (TFT) can estimate the dynamic phasor magnitude and phase of a given number of harmonics too. Further improvements can be obtained if the fundamental signal frequency is estimated a priori [12, 13]. Indeed, in this way the coefficients of the linear system used for Taylor's series parameters estimation can be computed with better accuracy.

Another well-known signal processing approach (which is also suggested in the Annex D of the IEEE/IEC Standard 60255-118-1:2018 [14]) is the so-called direct Down-Conversion and Filtering (DCF) method. This approach relies on the amplitude demodulation of the in-phase and quadrature components of the acquired digitized voltage and current signals followed by two Low-Pass Filters (LPFs) acting in parallel. The DCF method retains the amplitude and phase oscillations occurring in a given bandwidth, while removing the image of the fundamental as well as possible harmonics, interharmonics and part of the broadband noise floor. Therefore, the specifications of the LPFs and the related design procedure are of vital importance to ensure that the performance of the DCF method is compliant with the P Class or M Class requirements of the Standard. Generally, the Finite Impulse Response (FIR) filters are used to this purpose, partly because both their design is quite flexible and their phase response can be linear, so avoiding phase distortion. Thus, an FIR filter with a two-cycle-long triangular impulse response is reported, as an example, in the Annex D of the IEEE/IEC Standard for P class PMUs [15]. However, such a filter can provide a good harmonics rejection only when the fundamental frequency is very close to the nominal value (i.e., 50/60 Hz), while the pass-band and stop-band specifications are not considered at all. In the presence of off-nominal frequency deviations, a high rejection of harmonics can be achieved by using adaptive filtering techniques [16]. A filter design mask for potential M Class filters is proposed in [17]. Some conservative LPF filter design criteria for PMUs are also described in [18]. The underlying idea of such criteria is

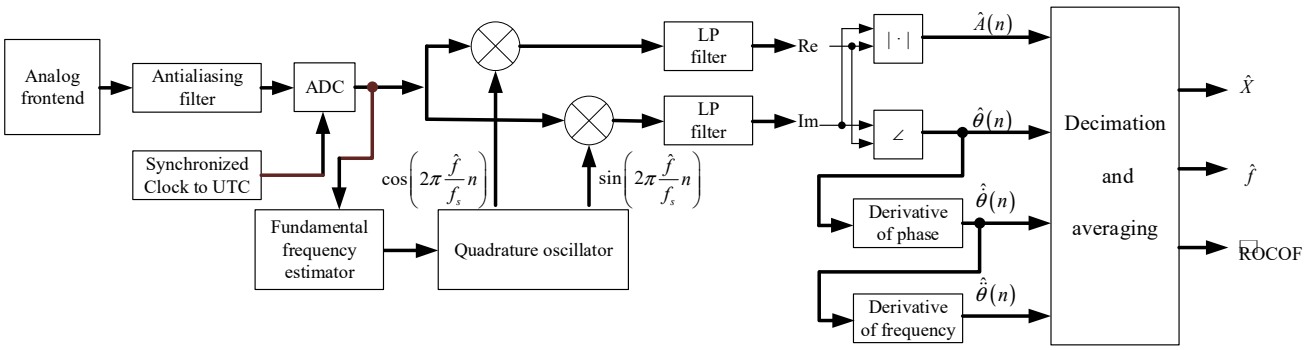


Fig. 1 - Block diagram of the DCF technique for synchrophasor, fundamental frequency and ROCOF estimation.

to preserve the dynamic synchrophasor amplitude and/or phase oscillations, while removing multiple narrowband interferers effectively. However, to the best of Authors' knowledge no deep research studies up to now have considered the problem of FIR filter design with the idea of mitigating the over- and undershoots, which instead may have a crucial impact in the most important scenario in which the P Class PMUs are supposed to be used, namely when sudden step-like changes occur [19]. To this regard, it is well known, that Gaussian filters exhibit no overshoot in the case of step-like input changes. However, Gaussian filters cannot be exactly implemented with finite difference equations, i.e., using digital filter design techniques. For this reason, two alternative approximated Gaussian filters for DCF-based synchrophasor estimation are proposed and compared in this paper. The former one relies on the windowing method, while the latter one relies on the cascade of multiple boxcar filters.

The rest of the paper is organized as follows. In Section II the general design criteria of the FIR approximated Gaussian filters are introduced. In Section III, the results of multiple simulation results in the P Class testing conditions specified in the IEEE/IEC Standard are reported and compared with the state of the art. Finally, Section IV concludes the paper.

## II. DCF METHOD BASED ON THE GAUSSIAN FILTER

### A. Synchrophasor estimation based on DCF

The synchrophasor of an ac waveform at nominal frequency $f_0$ is defined as a complex dynamic quantity, whose amplitude and phase angle at the UTC reference instants may change over time. The discrete-time signal acquired by the PMU with sampling rate $f_s=L\cdot f_0$ (where $L$ is an integer number) can be modeled as:

$$x(n)=A(n)\cos\left(2\pi\frac{f_0}{f_s}n+\theta(n)\right)+\eta(n)+\varepsilon(n) \quad (1)$$

where

$$\theta(n)=2\pi\frac{\Delta f}{f_s}n+\varphi(n), \quad (2)$$

$A(n)$ $\varphi(n)$ and $\Delta f$ represent the time-varying amplitude changes, the time-varying phase fluctuations and the frequency deviation of the fundamental component, respectively, while $\eta(n)$ and $\varepsilon(\cdot)$ represent the narrowband interferers (i.e., harmonics or interharmonics) and the wideband noise, respectively. Thus, the dynamic synchrophasor is defined as

$$X(n)=\frac{A(n)}{\sqrt{2}}e^{j\theta(n)}. \quad (3)$$

The block diagram related to the DCF estimation technique is shown in Fig. 1. This is in line with the approach suggested also in the Annex D of the IEEE/IEC Standard [14], although with some slight differences. The basic DCF technique assumes that the sampling signal frequency is disciplined by the synchronization module and that the sequence of acquired samples is mixed with two quadrature digital sinewaves. Two cascaded identical LPFs in parallel are then used to extract the in-phase (I) and quadrature (Q) components of the input ac waveform. Theoretically, a perfect frequency down-shifting of the fundamental to 0 Hz is obtained if the frequency of the signal generated by the digital quadrature oscillator is extracted from the input signal itself. As a result, LPFs with a narrower passband and a more relaxed transition band can be used, as explained in [18]. Frequency estimation and sinewave synthesis can be done in variety of ways, most notably through a Phase-Locked Loop (PLL), which however may suffer from unpredictable oscillations and stability problems during transients, due to its inherent nonlinearity. For this reason, in this paper the same IpDFT estimator with the Hann window adopted in [18] is used. This estimator relies on the two largest spectral samples around the frequency bin of the fundamental component and it exploits the analytical expressions that hold in the Hann window case to estimate possible off-nominal frequency deviations and, accordingly, to update the actual frequency of the quadrature oscillator sample by sample. In the DCF approach, the LPFs outputs provide an estimate of the real and imaginary parts of the dynamic phasor (3). Therefore, they can be used to easily derive the phasor magnitude $\hat{A}(n)$ and phase $\hat{\varphi}(n)$. In accordance with the IEEE/IEC Standard, the fundamental frequency and its ROCOF can instead be tracked over time by using the 1st-order and the 2nd-order Euler finite difference of the phase angles updated sample by sample, i.e.

$$\hat{f}(n)=f_0+\frac{f_s}{4\pi}\left(\hat{\theta}(n+1)-\hat{\theta}(n-1)\right) \quad (4)$$

$$\hat{\mathrm{ROCOF}}(n)=\frac{f_s^2}{2\pi}\left(\hat{\theta}(n+1)-2\hat{\theta}(n)+\hat{\theta}(n-1)\right) \quad (5)$$

However, when the output stream of synchrphasor data is decimated to be transferred to the Phasor Data Concentrator, it is recommended to average the values returned by (4) and (5) over subsequent, disjoint intervals of duration $1/RR$ (with $RR$ being the Reporting Rate) to reduce the random noise variance.

### B. General design criteria of the Gassian filter

As known, the LPFs used for synchrophasor estimation have to meet tight specifications to avoid that the spectral leakage and the limited attenuation of possible out-of-band interferers may excessively degrade synchrophasor estimation. To address such requirements, the problem of overshoot minimization during transients has been often overlooked in the literature. In the IEEE/IEC Standard the limits on overshoot are rather loose, i.e. 5% or 10% of step size for P Class and M Class PMUs, respectively. The overshoot size also typically affects the settling time and, indirectly, the response time. In principle, a Gaussian filter ensures zero overshoot with minimal rise and fall times when a step-like variation is considered. The impulse response and the Fourier Transform of an ideal Gaussian filter are

$$g(t,\sigma_t)=\frac{1}{\sqrt{2\pi}\sigma_t}e^{-\frac{t^2}{2\sigma_t^2}} \xrightarrow{F} G(f,\sigma_t)=e^{-\pi^2\sigma_t^2 f^2}, \quad (6)$$

where $t$ and $f$ are the time variable (expressed in s) and the frequency variable (expressed in Hz), respectively. Assuming that the fundamental frequency is downshifted around 0 Hz, the LPF passband and stopband edges (denoted as $f_{PB}$ and $f_{SB}$, respectively) should take the values reported in [18], i.e., $f_{PB}$ = 4.2 Hz and $f_{SB}$ = 48 Hz, respectively. This is essential to ensure a good tracking capability of amplitude and phase oscillations, while adequately rejecting the spectral leakage of the fundamental image component, the low-order harmonics and the wideband noise floor. However, the behavior of an ideal Gaussian filter depends on parameter $\sigma_t$ only. Therefore, in the case at hand, the value of $\sigma_t$ has to be set small enough to make the worst-case Total Vector Error (TVE) lower than the most conservative limit reported in the IEEE/IEC Standard, i.e. $TVE_{max}$ = 1%. By replacing the analytical expression of the frequency response of the Gaussian filter in (6) into the upper bound expression for the *TVE* reported in [18], after a few algebraic steps it results easily that

$$\begin{aligned} TVE(\sigma_t) \le & \frac{1-G(f_{PB},\sigma_t)}{2}+\frac{G(f_2,\sigma_t)}{2} \\ & +U_H\sum_{h=1}^{H-1}G(f_h,\sigma_t)+\sqrt{\frac{46}{SNR}\frac{f_{PB}}{f_s}} < TVE_{\max} \end{aligned} \quad (7)$$

where $f_h$ for $h$ = 1, …, $H$-1 (with $H \le 50$) are the harmonic frequencies after mixing the input signal with the quadrature sinewaves, $U_H$ is the maximum allowed amplitude of all harmonics relative to the fundamental and *SNR* is the signal-to-noise ratio computed by considering only the fraction of white noise power within the antialiasing filter bandwidth. Assuming $f_0$=50 Hz, *SNR*=60 dB (in accordance with the experimental characterization reported in [20]), if the sampling frequency is in the order of a few kHz, it results from (7) that the lowest worst-case *TVE* value (quite smaller than 1%) is achieved for $\sigma_t \approx 6$ ms.

The main drawback of Gaussian filters is that they are inherently non-causal and they cannot be exactly implemented using finite difference equations. Thus, only approximate solutions with a different level of accuracy can be used. In addition, the existing Infinite Impulse Response (IIR) approximations, although more accurate than the FIR ones for $\sigma_t \cdot f_s$ values greater than 3 [21], can hardly process streams of data in real-time. For this reason, in the following two alternative FIR-based approximate solutions are considered. The former one is obtained with the windowing method. The latter one results instead from the cascade of multiple boxcar filters. To make the maximum and mean square truncation errors between the impulse response of the ideal Gaussian filter and the approximated FIR solutions as small as possible, the FIR impulse response length should be $N \ge 6\sigma_t \cdot f_s$, i.e., long enough to represent the Gaussian bell shape within the $\pm 3\sigma_t$ range. Of course, the value of $N$ cannot grow unboundedly in order not to make the response time of the filter excessively long. Notice that in the continuous-time domain a duration of $6\sigma_t$ corresponds to 36 ms, which is slightly less than 2 power line cycles at 50 Hz. This is the shortest possible duration of the impulse response of the digital FIR filter to keep the truncation error below an acceptable value.

In the following subsections, first the design steps of two alternative FIR Gaussian filters are described; then a quantitative comparison between the time and frequency features of the ideal Gaussian filter and the FIR approximations is provided.

### C. FIR approximated Gaussian filter design based on the windowing method

In general, the purpose of the windowing method is to choose a proper ideal frequency-selective filter (which always has a noncausal, infinite-duration impulse response) and then to window its ideal impulse response (properly shifting it in time) to obtain a linear-phase and causal FIR filter. In the case at hand, the impulse response of the FIR approximated Gaussian filter is

$$h_w(n)=g_d\left(n-\frac{N-1}{2},\sigma\right)w(n), \; n=0,\ldots,N\text{-}1 \quad (8)$$

where $w(n)$ is the chosen window function, $g_d(\,)$ denotes the discrete-time impulse response of the Gaussian filter obtained by sampling (6), $\sigma=\sigma_t \cdot f_s$ and $N$, without loss of generality is assumed to be an odd number. As known, in general the window function should be chosen in such a way that the maximum stopband or passband approximation error of the ideal frequency response is below a given threshold. However, in this paper, we are not interested in the worst-case approximation errors of the ideal frequency response, but rather in the lowest possible worst-case TVE values based on (7). In particular, the Discrete-Time Fourier Transform (DTFT) of (8) using a Kaiser's window of $N \ge 6\sigma_t \cdot f_s$ =180 samples (assuming that $f_s$=5 kHz for the reasons explained in Section II.E) was computed and replaced to $G(\cdot,\cdot)$ into (7). The value of the window parameter $\beta$ (which defines the window shape and its spectral characteristics) was swept linearly within a reasonably broad range (i.e., from 0 to 5) to find heuristically the value that minimizes the worst-case TVE, assuming that $H$=50 (with the relative amplitude of all harmonics being $U_H$=1%), *SNR*=60 dB, $f_{PB}$ = 4.2 Hz and $TVE_{\max}$=1% in (7). Surprisingly, for short impulse responses (e.g., with length in the order of 2 power line cycles), the best results were obtained for $\beta \approx 0$, i.e. when an almost rectangular window is used. This is due to the fact that the errors occurring in the transition band due to the wider spectral main-lobe of a Kaiser's window with a larger $\beta$ value tend to prevail over the benefits of decreasing the spectrum side-lobe magnitude and, consequently, over the residual interference of the harmonics at the output of the filter.

### D. FIR approximated Gaussian filter design based on cascaded boxcar filters

Another way to implement an approximated FIR Gaussian filter is through the cascade of multiple boxcar filters [22]. A boxcar filter of length $M$ is just a plain moving average filter whose impulse and frequency responses are given respectively by

$$h_b(n) = \begin{cases} \dfrac{1}{M}, & 0 \le n \le M-1 \\ 0, & \text{elsewhere} \end{cases}, \tag{9}$$

$$H_b\left(e^{j\omega}\right) = e^{-j\omega(M-1)/2}\,\frac{\sin\left(\omega M/2\right)}{M\sin\left(\omega/2\right)}. \tag{10}$$

where $\omega$ denotes the normalized angular frequency. If $K$ is the number of cascaded boxcar filters, the overall impulse response $h_{bK}(n)$ is given by the convolution of $K$ impulse responses defined as in (9). Thus, the total length of the FIR filter is $N = KM - K + 1$, and its frequency response is

$$H_{bK}\left(e^{j\omega}\right) = e^{-j\omega(N-1)/2}\,\frac{\sin^K\left(\omega M/2\right)}{M^K\sin^K\left(\omega/2\right)}. \tag{11}$$

If (9) is regarded as the Probability Density Function (PDF) of a uniform random variable, its standard deviation is $\sqrt{\left(M^2-1\right)/12}$. Due to the Central Limit Theorem (CLT), the PDF resulting from the convolution of $K$ PDFs expressed as in (9) tends to exhibit a Gaussian shape with variance that grows by a factor $K$. Thus, $h_{bK}(n)$ tends to be Gaussian with standard deviation $\sqrt{K\left(M^2-1\right)/12}$ [22]. It is interesting to observe that the filter with a triangular impulse response mentioned in the Annex D of the IEEE/IEC Standard for P Class PMUs (which will be also considered for comparison in Section III) can indeed be regarded as a special case of a cascaded boxcar filter with $K$=2. However, better results can be achieved if the values of $M$ and $K$ are computed by solving the following optimization problem, i.e.

$$\min_{M,K}\left|\sqrt{K\left(M^2-1\right)/12} - \sigma_t f_s\right| \tag{12}$$

such that $KM - K + 1 = T_O f_s$, where $T_O$ is the wanted observation interval duration. Since variables $K$ and $M$ can just take integer values, the set of possible solutions includes a finite number of elements. Therefore, the best pair of ($K$, $M$) values can be found through exhaustive search, by replacing (11) to $G(\cdot,\cdot)$ into (7), and by checking a posteriori if the constraint on $TVE_{\max}$ is still met in the very same conditions described in Section II.C.

### E. Filters characteristics comparison

Assuming that the sampling frequency $f_s$ is set to 5 kHz (i.e., large enough to avoid aliasing due to harmonics if a suitable anti-aliasing filter is used), the length of the FIR filters for $\sigma_t$ = 6 ms should be $N \ge 180$, as shown in Section II.C. However, the best solution to the cascaded boxcar filters optimization problem assuming an overall impulse response of length of about 2 cycles was obtained for $K$=4 and $M$ = 52. Therefore, to enable a fair comparison of the two alternative FIR approximate Gaussian filters considered in this paper, $N$ = 205 coefficients (i.e., slightly more than 2 power line cycles) were used in both cases.

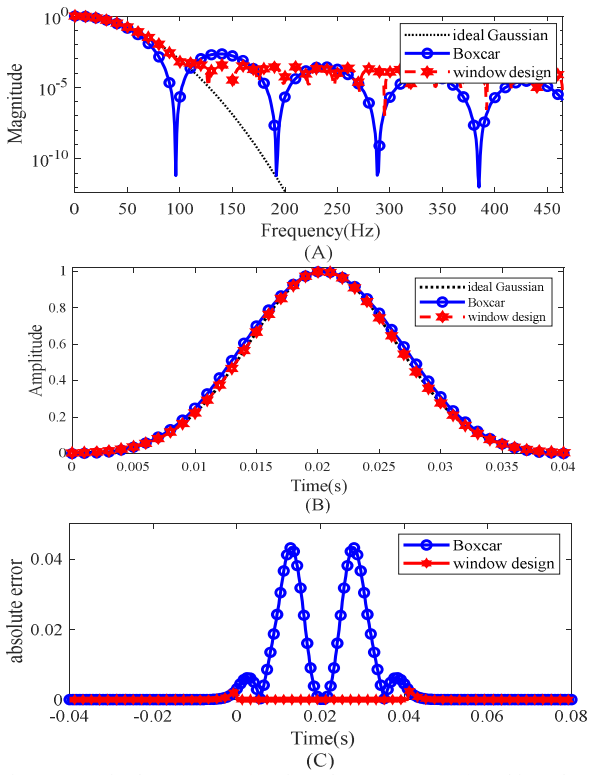


Fig. 2. Magnitude responses (A), impulse responses (B) and impulse response absolute error (C) of the FIR approximated solutions implemented approximately over 2 nominal power line cycles with the windowing method and by cascading 4 boxcar filters.

The magnitude and impulse responses of the Gaussian filter of both FIR solutions as well as the absolute approximation errors in the time domain are shown in Fig. 2(A)-(C), respectively. Fig. 2(A) shows that both filters approximate the Gaussian frequency response with high accuracy in the passband. The magnitude responses of both FIR filters in the stopband instead differ considerably from the ideal one. This behavior was expected and it is due partly to the presence of zeros in the FIR filters transfer functions and partly to the obvious impossibility to model an exponentially decreasing decay through polynomials. The boxcar filter decades slightly faster than the ideal Gaussian in the passband. In the stopband, the magnitude response of the cascaded boxcar filter exhibits deeper notches than in the case of the FIR filter designed with the windowing method, especially around 100 Hz. This indicates that the solution based on the cascaded boxcar filters provides a better suppression of the fundamental image component, which is notoriously quite critical when short observation intervals are considered [23].

The impulse responses in Fig. 2(B) and above all the related time-domain absolute approximation errors plotted in Fig. 2(C) show that the windowing method provides a better approximation of the ideal Gaussian function than the chosen four-stage cascaded boxcar filter. Indeed, the Root Mean Square (RMS) errors are $4.3\times10^{-5}$and $1.6\times10^{-3}$, respectively.

## III. Simulations and Results

To evaluate the estimation accuracy of the DCF estimator based on the FIR approximated Gaussian filters designed as described in Section II and to compare their performance with those obtained with the triangular impulse response filter

TABLE I –MAXIMUM TVE, |FE| AND |RFE| VALUES OBTAINED WITH THE DCF ESTIMATOR AND THE TWO ALTERNATIVE FIR APPROXIMATED GAUSSIAN FILTERS DESIGNED AS EXPLAINED IN SECTION II OR IEEE/IEC THE FILTER WITH A TRIANGULAR IMPULSE RESPONSE SUGGESTED IN THE ANNEX D OF THE IEEE/IEC STANDARD. THE IMPULSE RESPONSE OF ALL FILTERS IS ABOUT 2 NOMINAL CYCLES LONG THE TESTS ARE SPECIFIED IN THE IEC/IEEE STANDARD 60255-118-1. IN ALL CASES, A NOISE FLOOR SUCH THAT *SNR* = 60 DB IS ASSUMED. THE P CLASS LIMITS SPECIFIED IN THE IEEE/IEC STANDARD ARE ALSO SHOWN FOR THE SAKE OF COMPARISON.

| | **Max. *TVE* (%)** | | | | **Max. \|*FE*\| (mHz)** | | | | **Max. \|*RFE*\| (Hz/s)** | | | |
|---|---|---|---|---|---|---|---|---|---|---|---|---|
| **Test case** | **Std. limit** | **Windowing method** | **Cascaded boxcar filters** | **Triangular filter** | **Std. limit** | **Windowing method** | **Cascaded boxcar filters** | **Triangular filter** | **Std. limit** | **Windowing method** | **Cascaded boxcar filters** | **Triangular filter** |
| *a* | 1 | 0.12 | 0.08 | 0.83 | 5 | 6.5 | 6.2 | 11.7 | 0.4 | 1.7 | 0.69 | 6.18 |
| *b* | 1 | 0.25 | 0.19 | 0.83 | 5 | 8.1 | 6.5 | 13.1 | 0.4 | 2.5 | 1.27 | 6.38 |
| *c* | 3 | 0.12 | 0.08 | 0.19 | 60 | 5.8 | 5.7 | 3.9 | 2.3 | 0.68 | 0.40 | 0.66 |
| *d* | 3 | 0.11 | 0.07 | 0.42 | 60 | 5.4 | 5.6 | 5.6 | 2.3 | 0.69 | 0.41 | 0.70 |

TABLE II –MAXIMUM SYNCHROPHASOR, FREQUENCY AND ROCOF RESPONSE TIME OBTAINED WITH THE DCF ESTIMATOR AND THE TWO ALTERNATIVE FIR APPROXIMATED GAUSSIAN FILTERS DESIGNED AS EXPLAINED IN SECTION II OR IEEE/IEC THE FILTER WITH A TRIANGULAR IMPULSE RESPONSE SUGGESTED IN THE ANNEX D OF THE IEEE/IEC STANDARD. THE IMPULSE RESPONSE OF ALL FILTERS IS ABOUT 2 NOMINAL CYCLES LONG. THE P CLASS LIMITS SPECIFIED IN THE IEEE/IEC STANDARD ARE ALSO SHOWN FOR THE SAKE OF COMPARISON.

| | **Synchrophasor response time(cycles)** | | | | **Frequency response time(cycles)** | | | | **ROCOF response time(cycles)** | | | |
|---|---|---|---|---|---|---|---|---|---|---|---|---|
| **Test case** | **Std. limit** | **Windowing method** | **Cascaded boxcar filters** | **Triangular filter** | **Std. limit** | **Windowing method** | **Cascaded boxcar filters** | **Triangular filter** | **Std. limit** | **Windowing method** | **Cascaded boxcar filters** | **Triangular filter** |
| *e* | 2 | 1.75 | 1.75 | 1.79 | 4.5 | 2.6 | 2.5 | 2.8 | 6 | 3.1 | 3 | 3.2 |
| *f* | 2 | 1.75 | 1.75 | 1.79 | 4.5 | 2.6 | 2.5 | 2.8 | 6 | 3.1 | 3 | 3.2 |

suggested in the Annex D of the IEEE/IEC Standard, multiple Monte Carlo simulations were performed in various P Class testing conditions specified in [14], i.e.

- *Case a*: considering off-nominal frequency deviations ranging from -2 Hz to 2 Hz;
- *Case b*: considering off-nominal frequency deviations ranging from -2 Hz to 2 Hz, and including one harmonic at a time from the 2nd up to the 50th one, with amplitude equal to 1% of the fundamental.
- *Case c*: considering a sinusoidal Amplitude Modulation (AM) with modulation index equal to 0.1 and modulating tone frequency up to 2 Hz.
- *Case d:* considering a phase modulation (PM) with modulation index 0.1 rad and modulating tone frequency up to 2 Hz.
- *Case e*: considering ±10% amplitude step changes.
- *Case f*: considering ±π/18 phase step changes.

In all the testing conditions listed above, 50 waveforms of at least 2 s each were generated. The initial phase of the fundamental component is increased linearly from 0 to 2π. The sampling frequency $f_s$ is set to be 5 kHz with the output results decimated cycle by cycle, assuming that the reporting rate is 50 frame/s. To make the simulation results more realistic, white Gaussian noise with zero mean and variance such that *SNR*=60 dB was added to all data records. The maximum Total Vector Errors (TVE), the absolute Frequency Errors (|FE|) and the absolute ROCOF Errors (|RFE|) obtained over repeated simulations in the testing conditions labeled as *Case a* to *d* are reported Table I, where they are also compared with the results obtained when the DCF technique is used with the P Class triangular impulse response filter mentioned in the Standard. The response time values in *Cases e* and *f* obtained using the same LPFs are instead reported in Table II. The IEEE/IEC Standard limits for a reporting rate of 50 frames/s are also shown for the sake of comparison.

As shown in Table I, the accuracy of the DCF method with the two alternative FIR approximated Gaussian filters is generally better than in the case when the filter with the triangular impulse response is used. Also, the accuracy of both the approximated Gaussian filters is quite comparable in all testing conditions with a slight preference for the cascaded boxcar filter solution. The TVE limits are met in all cases. The FE and RFE values show that in some P Class testing conditions the DCF estimator is not able to meet the requirements of the IEEE/IEC Standard. However, this is not due to the designed filters, but rather to the Euler-based estimators used to compute the first and second derivative of the phase angle. Even if the one-cycle average inside the output decimator tends mitigate this problem, no criteria are currently applied to keep FE and RFE under control. In fact, further filter design criteria should be applied to this purpose. The response time obtained with both FIR filters in the case of amplitude or phase steps are almost the same. Also, they are lower than those achieved with the filter with a triangular impulse response and meet the limits specified in the IEEE/IEC Standard.

To demonstrate the effectiveness of both design strategies to mitigate the overshoots, the estimated amplitude and phase values during two positive step changes in the *Case* e and *f* are shown in Fig. 3. The curves in Fig. 3 confirm that both FIR approximated Gaussian filter as well as the triangular filter ensure a negligible overshoot, as expected. The small fluctuations before and after the step change are mainly due to the infiltration of the image component of the fundamental, which cannot be filtered out completely. To further investigate the effect of possible step-like changes, the tests of *Cases e* and *f* were repeated by increasing linearly the angle at which the steps occur from 0 to 2π. The maximum undershoot and overshoot values at the pre- and post-transition times (denoted as $t_{pre}$ and $t_{post}$) defined in the IEEE/IEC Standard are shown in Table III. Clearly, such values are minor and they are strongly influenced by the infiltration of the image component of the fundamental, as already explained above.

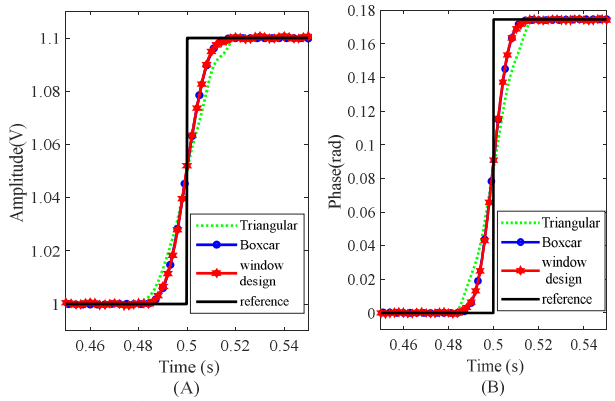


Fig. 3. Estimated phasor amplitude during an amplitude step change (A), and estimated phasor angle during a phase step change (B).

TABLE III – MAXIMUM ABSOLUTE OVERSHOOT AND UNDERSHOOT VALUES OBTAINED WITH THE DCF ESTIMATOR AND THE TWO ALTERNATIVE FIR APPROXIMATED GAUSSIAN FILTERS AT THE PRE- AND POST-TRANSITION TIMES OF REPEATED AMPLITUDE AND PHASE STEP CHANGES OCCURRING WHEN THE FUNDAMENTAL PHASE RANGES FROM 0 TO 2 $\pi$. THE VALUES ARE RELATIVE TO THE STEP MAGNITUDE.

| | **Amplitude step** | | **Phase step** | |
|---|---|---|---|---|
| **Windowing method** | $t_{pre}$ | $t_{post}$ | $t_{pre}$ | $t_{post}$ |
| | 1% | 1% | 0.5% | 0.5% |
| **Cascaded boxcar filters** | $t_{pre}$ | $t_{post}$ | $t_{pre}$ | $t_{post}$ |
| | 0.5% | 0.4% | 0.3% | 0.3% |

## IV. CONCLUSIONS

In this paper, two alternative FIR approximated Gaussian filter (based on the windowing method and on multiple cascaded boxcar filters, respectively) are used to estimate the synchrophasor magnitude and phase through the direct Down-Conversion and Filtering (DCF) technique. The rationale of this study is to ensure compliance with the P Class IEEE/IEC Standard requirements, while avoiding estimation overshoots during the transients associated with step-like events. Both filters rely on a common criterion for ideal Gaussian filter design, followed by a specific optimization procedure to maximize filter performance when impulse responses of about two power line cycles are considered. Both implementations are able to adequately preserve dynamic synchrophasor amplitude or phase oscillations and to remove harmonics and noise. The results of amplitude and phase step tests confirm that the overshoot is negligible. Even though the windowing method provides a better approximation of the Gaussian impulse response, the accuracy of the DCF technique with the cascaded boxcar filter is slightly better because the image component of the fundamental is better suppressed. Unfortunately, the accuracy of frequency and ROCOF estimation is limited by the Euler-based method suggested in the IEEE/IEC Standard to compute the first and second derivative of the instantaneous phase. Further studies are currently ongoing to design approximate Gaussian derivative filters which could provide more accurate frequency and ROCOF estimates with zero overshoot as well.

## ACKNOWLEDGMENT

This work was supported by the science and technology innovation Program of Hunan Province under Grant 2021RC4020 and by the China Scholarship Council.

## REFERENCES

[1] A. Borghetti, C. A. Nucci, M. Paolone, G. Ciappi, and A. Solari, "Synchronized Phasors Monitoring During the Islanding Maneuver of an Active Distribution Network," *IEEE Trans. on Smart Grid,* vol. 2, no. 1, pp. 82-91, 2011.

[2] D. Macii, D. Belega, and D. Petri, "IpDFT-Tuned Estimation Algorithms for PMUs: Overview and Performance Comparison," *Applied Sciences,* vol. 11, no. 5, p. 2318, 2021.

[3] J. Liu, J. Tang, F. Ponci, A. Monti, C. Muscas, and P. A. Pegoraro, "Trade-Offs in PMU Deployment for State Estimation in Active Distribution Grids," *IEEE Trans. on Smart Grid,* vol. 3, no. 2, pp. 915-924, 2012.

[4] H. Wen, J. Zhang, W. Yao, and L. Tang, "FFT-Based Amplitude Estimation of Power Distribution Systems Signal Distorted by Harmonics and Noise," *IEEE Trans. on Industrial Informatics,* vol. 14, no. 4, pp. 1447-1455, Apr 2018.

[5] F. J. Harris, "On the use of windows for harmonic analysis with the discrete Fourier transform," *Proceedings of the IEEE,* vol. 66, no. 1, pp. 51-83, 1978.

[6] A. Derviškadić, P. Romano, and M. Paolone, "Iterative-Interpolated DFT for Synchrophasor Estimation: A Single Algorithm for P- and M-Class Compliant PMUs," *IEEE Trans. on Instr. and Meas.,* vol. 67, no. 3, pp. 547-558, 2018.

[7] T. Grandke, "Interpolation Algorithms for Discrete Fourier Transforms of Weighted Signals," *IEEE Trans. on Instr. and Meas.,* vol. 32, no. 2, pp. 350-355, 1983.

[8] M. D. Sacchi, T. J. Ulrych, and C. J. Walker, "Interpolation and extrapolation using a high-resolution discrete Fourier transform," *IEEE Trans. on Signal Processing,* vol. 46, no. 1, pp. 31-38, 1998.

[9] J. A. d. l. O. Serna, "Dynamic Phasor Estimates for Power System Oscillations," *IEEE Trans. on Instr. and Meas.,* vol. 56, no. 5, pp. 1648-1657, 2007.

[10] D. Petri, D. Fontanelli, and D. Macii, "A Frequency-Domain Algorithm for Dynamic Synchrophasor and Frequency Estimation," *IEEE Trans. on Instr. and Meas.,* vol. 63, no. 10, pp. 2330-2340, 2014.

[11] D. Belega, D. Fontanelli, and D. Petri, "Dynamic Phasor and Frequency Measurements by an Improved Taylor Weighted Least Squares Algorithm," *IEEE Trans. on Instr. and Meas.,* vol. 64, no. 8, pp. 2165-2178, Aug 2015.

[12] P. Castello, R. Ferrero, P. A. Pegoraro, and S. Toscani, "Space Vector Taylor–Fourier Models for Synchrophasor, Frequency, and ROCOF Measurements in Three-Phase Systems," *IEEE Trans. on Instr. and Meas.,* vol. 68, no. 5, pp. 1313-1321, 2019.

[13] R. Ferrero, P. A. Pegoraro, and S. Toscani, "Synchrophasor Estimation for Three-Phase Systems Based on Taylor Extended Kalman Filtering," *IEEE Trans. on Instr. and Meas.,* vol. 69, no. 9, pp. 6723-6730, 2020.

[14] "IEEE/IEC International Standard - Measuring relays and protection equipment - Part 118-1: Synchrophasor for power systems - Measurements," *IEC/IEEE 60255-118-1:2018,* pp. 1-78, 2018.

[15] "IEEE Standard for Synchrophasor Measurements for Power Systems," *IEEE Std C37.118.1-2011 (Revision of IEEE Std C37.118-2005),* pp. 1-61, 2011.

[16] A. J. Roscoe, I. F. Abdulhadi, and G. M. Burt, "P and M Class Phasor Measurement Unit Algorithms Using Adaptive Cascaded Filters," *IEEE Transactions on Power Delivery,* vol. 28, no. 3, pp. 1447-1459, 2013.

[17] A. J. Roscoe, B. Dickerson, and K. E. Martin, "Filter Design Masks for C37.118.1a-Compliant Frequency-Tracking and Fixed-Filter M-Class Phasor Measurement Units," *IEEE Trans. on Instr. and Meas.,* vol. 64, no. 8, pp. 2096-2107, 2015.

[18] D. Macii and D. Petri, "Digital Filters for Phasor Measurement Units: Design Criteria, Advantages and Limitations," in *2019 IEEE 10th Int. Workshop on Applied Meas. for Power Systems (AMPS)*, 2019, pp. 1-6.

[19] D. Macii and D. Petri, "Rapid Voltage Change Detection: Limits of the IEC Standard Approach and Possible Solutions," *IEEE Trans. on Instr. and Meas.,* vol. 69, no. 2, pp. 382-392, 2020.

[20] M. Luiso, D. Macii, P. Tosato, D. Brunelli, D. Gallo, and C. Landi, "A Low-Voltage Measurement Testbed for Metrological Characterization of Algorithms for Phasor Measurement Units," *IEEE Trans. on Instr. and Meas.,* vol. 67, no. 10, pp. 2420-2433, Oct 2018.

[21] D. Hale, "Recursive gaussian filters," *CWP-546,* 2006.

[22] W. M. Wells, "Efficient Synthesis of Gaussian Filters by Cascaded Uniform Filters," *IEEE Trans. on Pattern Analysis and Machine Intelligence,* vol. PAMI-8, no. 2, pp. 234-239, 1986.

[23] D. Macii, D. Petri, and A. Zorat, "Accuracy Analysis and Enhancement of DFT-Based Synchrophasor Estimators in Off-Nominal Conditions," *IEEE Trans. on Instr. and Meas.,* vol. 61, no. 10, pp. 2653-2664, Oct 2012.